*Int. J. Electrochem. Sci.*, 14 **(2019)** 6009 – 6017, doi: 10.20964/2019.07.41

International Journal of
ELECTROCHEMICAL
SCIENCE
www.electrochemsci.org

*Short Communication*

# The Intermediate Temperature Electrochemical Properties of Silver and Aluminum Double-Doped Strontium Silicate

*Chang Wang, Ruifeng Du, Yan Han, Hongtao Wang*[*]

School of Chemical and Material Engineering, Fuyang Normal University; Anhui Provincial Key Laboratory for Degradation and Monitoring of Pollution of the Environment, Fuyang 236037, China
[*]E-mail: hwang@fync.edu.cn

*Received:* 4 March 2019/ *Accepted:* 5 May 2019 / *Published:* 10 June 2019

In this study, $Sr_{0.6}Ag_{0.4}SiO_{3-\alpha}$ and $Sr_{0.6}Ag_{0.4}Si_{0.9}Al_{0.1}O_{3-\alpha}$ electrolytes were synthesized via a high temperature solid state reaction method using $SrCO_3$, $SiO_2$, $AgNO_3$ and $Al_2O_3$ as raw materials. The phase purities and morphologies of $Sr_{0.6}Ag_{0.4}SiO_{3-\alpha}$ and $Sr_{0.6}Ag_{0.4}Si_{0.9}Al_{0.1}O_{3-\alpha}$were confirmed by X-ray diffractometer and scanning electron microscopy. SEM photos showed that $Sr_{0.6}Ag_{0.4}SiO_{3-\alpha}$ and $Sr_{0.6}Ag_{0.4}Si_{0.9}Al_{0.1}O_{3-\alpha}$ pellets were well-sintered. The Arrhenius plots indicated that the activation energies of $Sr_{0.6}Ag_{0.4}SiO_{3-\alpha}$ and $Sr_{0.6}Ag_{0.4}Si_{0.9}Al_{0.1}O_{3-\alpha}$ are 107.3 ± 3.2 $kJ\cdot mol^{-1}$ and 107.7 ± 2.1 $kJ\cdot mol^{-1}$in nitrogen atmosphere from 400 °C to 800 °C, respectively. $Sr_{0.6}Ag_{0.4}SiO_{3-\alpha}$ showed the highest maximum power density of 48.5 $mW\cdot cm^{-2}$at 800 °C.

**Keywords:** Electrolyte; Fuel cell; Conductivity; Strontium silicate

## 1. INTRODUCTION

Solid oxide fuel cells (SOFCs) are considered to be promising energy conversion devices, which not only have the characteristics of good fuel selectivity and no pollution, but also have very high energy-conversion efficiency [1-9]. Solid electrolytes play a key role in SOFCs by determining the conversion efficiency and working temperature. High operating temperature is a major challenge for solid electrolytes. Therefore, reducing the working temperature of an SOFC is a current research hotspot. The discovery of electrolyte materials with high conductivities at medium temperatures (400–800 °C) is of great significance [10-17].

In 2013, a composition of alkali metals-doped $SrSiO_3$ was reported as a new oxide ion electrolyte [18]. It is believed that $Na^+$ doping increases the conductivity due to the creation of interstitial oxide ions rather than oxide ion vacancies. The report attracted many researchers due to the electrolyte's excellent oxygen ion conductivity at 400–800 °C [19-28]. Yang et al. [25] prepared $Sr_{1-}$

$_x$Na$_x$SiO$_{3-x/2}$ ($x$=0.2, 0.3, 0.4, 0.45) materials by spark plasma sintering with high ion transference numbers of 0.99 at 500–600 °C, which met the requirement of being an SOFC electrolyte. Pandey [26] prepared a nominal composition of $Sr_{0.55}Na_{0.45}SiO_{2.775}$ by the solid state reaction route and found that it contained two crystalline phases, $SrSiO_3$ and the Na-rich phase identified as $Na_2Si_5O_5$. Therefore, the doping limit should be less than 45%.

Here, we try to use $Ag^+$ and $Al^{3+}$ double-doped $SrSiO_3$ to obtain a high conductivity at medium temperature. $Ag^+$ will be doped into the $SrSiO_3$ structure to replace the $Sr^{2+}$ due to the ionic radius of $Ag^+$ and $Sr^{2+}$ being closed, thus oxygen vacancy is introduced to improve the conductivity. On this basis, a double-doped structure is formed by doping $Al^{3+}$ ions into this structure (substitution of $Al^{3+}$ for $Si^{4+}$ to introduce oxygen vacancies). The double-doped structure will form more oxygen vacancies than the single-doped structure, thus, the conductivity will be significantly improved. In this paper, $Sr_{0.6}Ag_{0.4}SiO_{3-\alpha}$ and $Sr_{0.6}Ag_{0.4}Si_{0.9}Al_{0.1}O_{3-\alpha}$ electrolytes are reported. The structures, ionic conductivities and intermediate temperature electrical properties of the two samples are studied.

## 2. EXPERIMENTAL

$Sr_{0.6}Ag_{0.4}SiO_{3-\alpha}$ and $Sr_{0.6}Ag_{0.4}Si_{0.9}Al_{0.1}O_{3-\alpha}$ electrolytes were synthesized via a high temperature solid state reaction method using $SrCO_3$ (4.4289 g), $SiO_2$ (2.7036 g), $Ag_2O$ (2.32 g) and $Al_2O_3$ (0.2549 g) as raw materials. The reactant was mixed and ground for 5 h, then, sintered at 950 °C for 12 h. Samples were crushed and ground in a mortar, then, screened by a 200 mesh sieve. The samples were pressed into sheets and placed in a box furnace for a second calcination at 1000 °C for 12 h.

The phase purities of $Sr_{0.6}Ag_{0.4}SiO_{3-\alpha}$ and $Sr_{0.6}Ag_{0.4}Si_{0.9}Al_{0.1}O_{3-\alpha}$ were confirmed by X-ray diffractometer (XRD, X'pert Pro MPD, Holland's company, Amsterdam, Netherlands). The morphologies of the surface and cross sections of $Sr_{0.6}Ag_{0.4}SiO_{3-\alpha}$ and $Sr_{0.6}Ag_{0.4}Si_{0.9}Al_{0.1}O_{3-\alpha}$were observed using scanning electron microscopy (SEM, S-4700, Hitachi, Tokyo, Japan). The Sr, Ag, Si, Al and O elements of $Sr_{0.6}Ag_{0.4}SiO_{3-\alpha}$ and $Sr_{0.6}Ag_{0.4}Si_{0.9}Al_{0.1}O_{3-\alpha}$ were analyzed by energy-dispersive X-ray spectroscopy. For conductivity measurements, both side surfaces (area: 0.5 $cm^2$) of $Sr_{0.6}Ag_{0.4}SiO_{3-\alpha}$ and $Sr_{0.6}Ag_{0.4}Si_{0.9}Al_{0.1}O_{3-\alpha}$ (thickness: 1.0-1.1 mm) were coated in silver-palladium electrode paste and tested with an electrochemical analyzer (CHI660E, Chenhua, Shanghai, China) in a nitrogen at 400–800 °C. The conductivity vs. oxygen partial pressures ($pO_2$= $10^{-20}$ -1 atm) curve were measured at 800 °C. Finally, $H_2/O_2$ fuel cell performances of $Sr_{0.6}Ag_{0.4}SiO_{3-\alpha}$ and $Sr_{0.6}Ag_{0.4}Si_{0.9}Al_{0.1}O_{3-\alpha}$ were tested at 800 °C.

## 3. RESULTS AND DISCUSSION

Fig. 1 shows XRD patterns of $Sr_{0.6}Ag_{0.4}SiO_{3-\alpha}$ and $Sr_{0.6}Ag_{0.4}Si_{0.9}Al_{0.1}O_{3-\alpha}$. According to the results, $Sr_{0.6}Ag_{0.4}SiO_{3-\alpha}$ and $Sr_{0.6}Ag_{0.4}Si_{0.9}Al_{0.1}O_{3-\alpha}$ contain Ag (JCPDS 87-0720) phases in addition to the standard monoclinic $SrSiO_3$ (JCPDS 87-0474) structures. This shows that $Ag^+$ can't be as effective

as $Na^+$ [22-28] though its ionic radius is closed to $Sr^{2+}$. The diffraction peaks at 17.50º, 30.59º, 35.44º and 63.72 belong to the (002), (022), (004) and (044) of the perovskite structure of $SrSiO_3$, respectively.

The $Sr_{0.6}Ag_{0.4}SiO_{3-\alpha}$ and $Sr_{0.6}Ag_{0.4}Si_{0.9}Al_{0.1}O_{3-\alpha}$ external (a,c) and cross-sectional (b,d) SEM images are displayed in Fig. 2. All photos have bright spots which are ascribed to the precipitated silver. A continuous, elongated crystalline microstructure is also observed. $Sr_{0.6}Ag_{0.4}SiO_{3-\alpha}$ and $Sr_{0.6}Ag_{0.4}Si_{0.9}Al_{0.1}O_{3-\alpha}$ pellets are well-sintered, and the grain boundaries are completely formed [23–25].

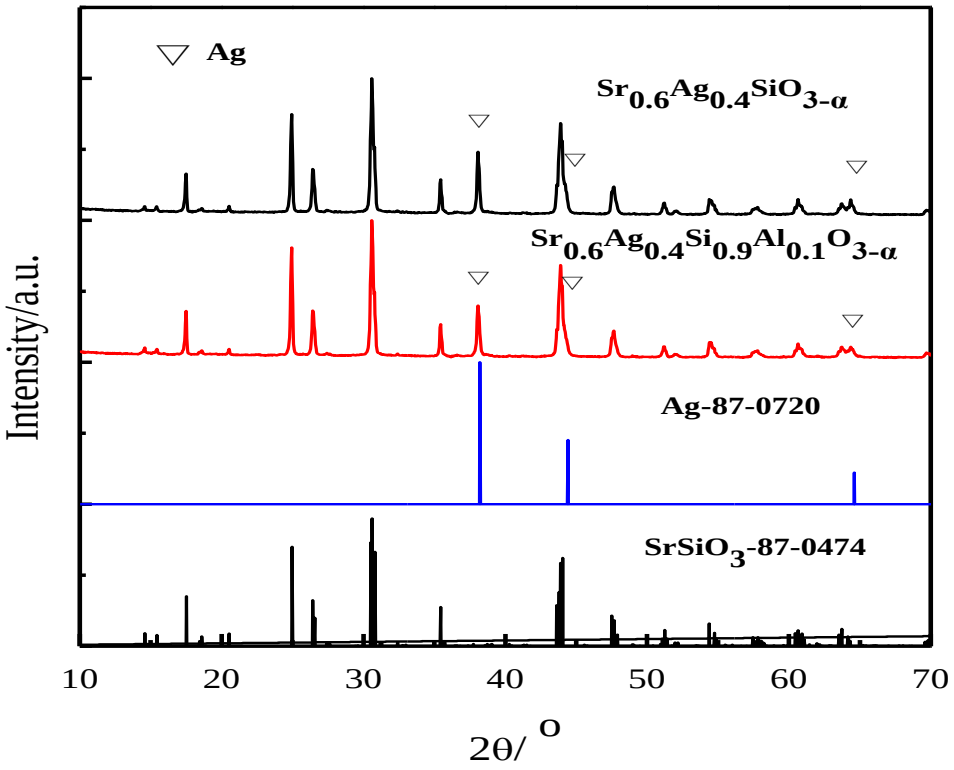


**Figure 1.** XRD patterns of $Sr_{0.6}Ag_{0.4}SiO_{3-\alpha}$ and $Sr_{0.6}Ag_{0.4}Si_{0.9}Al_{0.1}O_{3-\alpha}$.

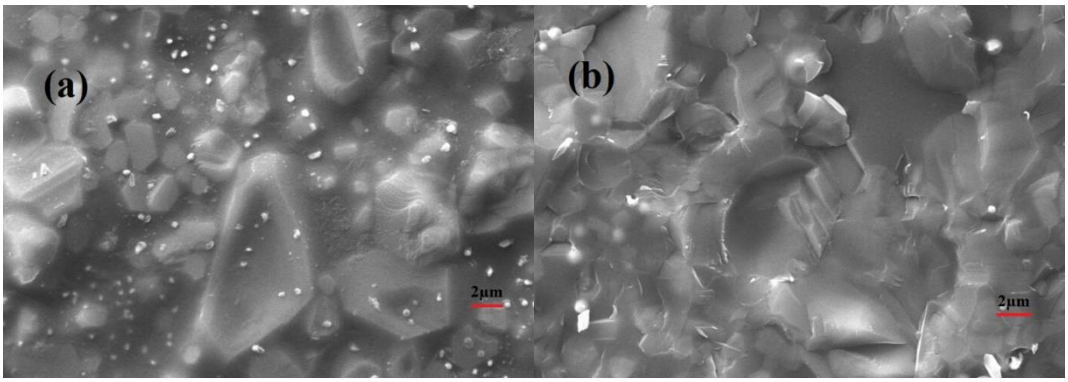

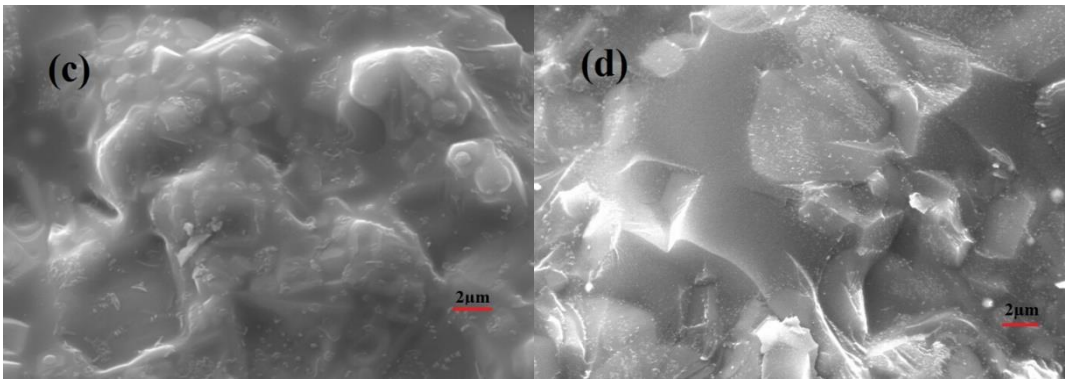


**Figure 2.**The SEM images of $Sr_{0.6}Ag_{0.4}SiO_{3-\alpha}$ and $Sr_{0.6}Ag_{0.4}Si_{0.9}Al_{0.1}O_{3-\alpha}$ external (a,c) and cross-sectional (b,d) surfaces.

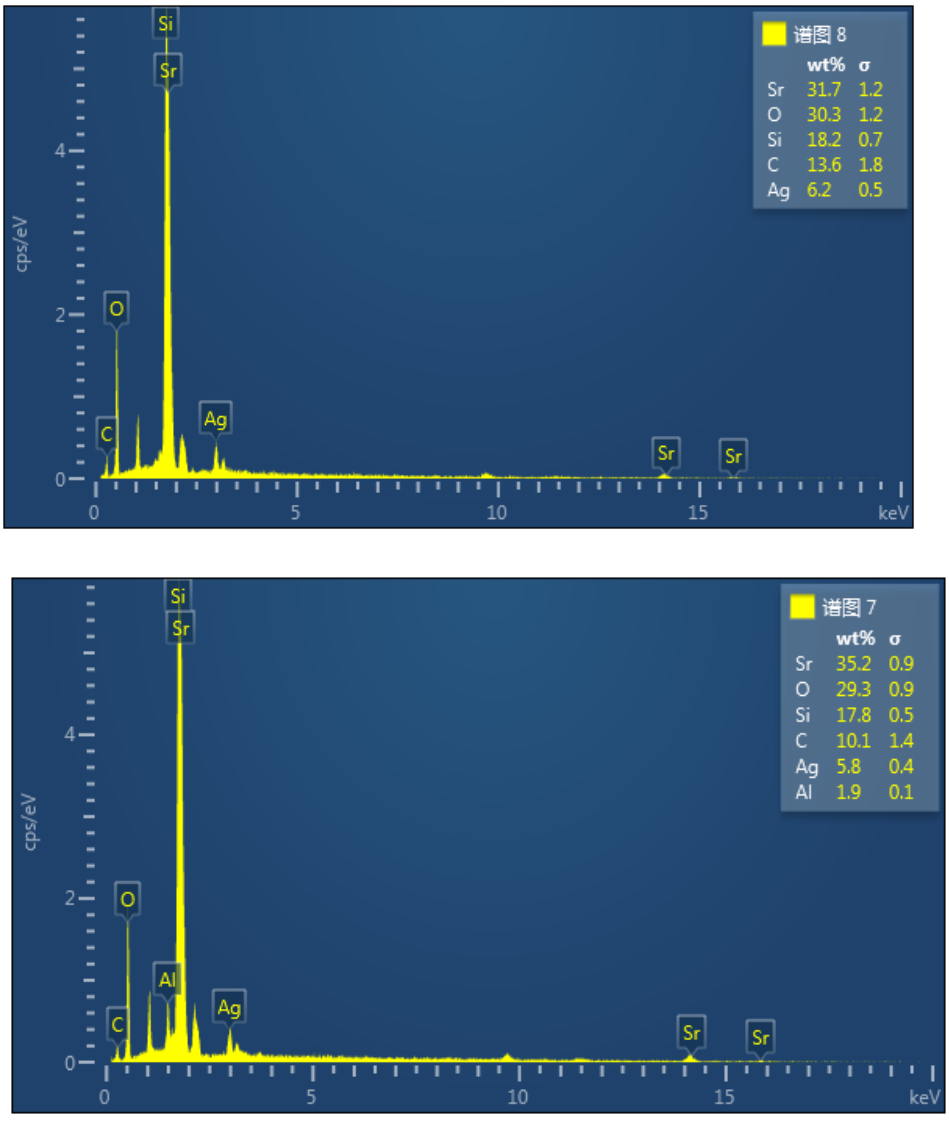


**Figure 3.**The energy-dispersive X-ray spectroscopy of Sr, Ag, Si, Al and O elements in $Sr_{0.6}Ag_{0.4}SiO_{3-\alpha}$ and $Sr_{0.6}Ag_{0.4}Si_{0.9}Al_{0.1}O_{3-\alpha}$.

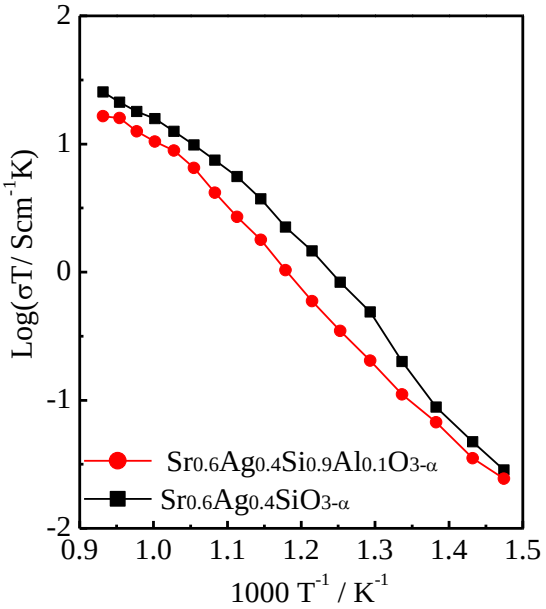


**Figure 4.**The conductivities of $Sr_{0.6}Ag_{0.4}SiO_{3-\alpha}$ and $Sr_{0.6}Ag_{0.4}Si_{0.9}Al_{0.1}O_{3-\alpha}$ vs. temperature in a nitrogen atmosphere from 400 °C to 800 °C.

The energy-dispersive X-ray analysis is displayed in Fig. 3. The spectrum contains four major peaks assigned to the Sr, Ag, Si and Al elements. The atomic ratios of Sr/Si and Al/Si are 0.56 and 0.11 which are close to the chemical composition of the molecular formula. However, Ag/Sr is far below the atomic ratios in the formula. This indicates that $Ag^+$ cannot be doped effectively, which is consistent with the results in Fig. 1 [22-28].

The Arrhenius plots of $Sr_{0.6}Ag_{0.4}SiO_{3-\alpha}$ and $Sr_{0.6}Ag_{0.4}Si_{0.9}Al_{0.1}O_{3-\alpha}$ vs. temperature in a nitrogen atmosphere from 400 °C to 800 °C are shown in Fig. 4. The slope indicates the activation energy of the sample. The activation energy of $Sr_{0.6}Ag_{0.4}Si_{0.9}Al_{0.1}O_{3-\alpha}$ is 107.7 ± 2.1 kJ·mol$^{-1}$, which slight higher than that of $Sr_{0.6}Ag_{0.4}SiO_{3-\alpha}$ (107.3 ± 3.2 kJ·mol$^{-1}$). The conductivity of $Sr_{0.6}Ag_{0.4}Si_{0.9}Al_{0.1}O_{3-\alpha}$ ($1.6\times10^{-2}$ S·cm$^{-1}$) is slightly higher than that of $Sr_{0.6}Ag_{0.4}SiO_{3-\alpha}$ ($2.4\times10^{-2}$ S·cm$^{-1}$) in a nitrogen atmosphere at 800 °C. And $Sr_{0.6}Ag_{0.4}SiO_{3-\alpha}$ and $Sr_{0.6}Ag_{0.4}Si_{0.9}Al_{0.1}O_{3-\alpha}$ show lower conductivities than those reported in the literature [18–19,25], which may be attributed to the existence of the second silver phase.

Fig. 5 shows the conductivities of $Sr_{0.6}Ag_{0.4}SiO_{3-\alpha}$ and $Sr_{0.6}Ag_{0.4}Si_{0.9}Al_{0.1}O_{3-\alpha}$ vs. oxygen partial pressures ($pO_2$= $10^{-20}$ -1 atm) at 800 °C. In the range of oxidative partial pressure, the log $\sigma \sim$ log $pO_2$ curve shows a horizontal straight line, which indicates that the samples show pure ionic conduction. Within the range of reductive partial pressure, the curves bend upward, indicating that the samples exhibit mixed conduction of ions and electrons.

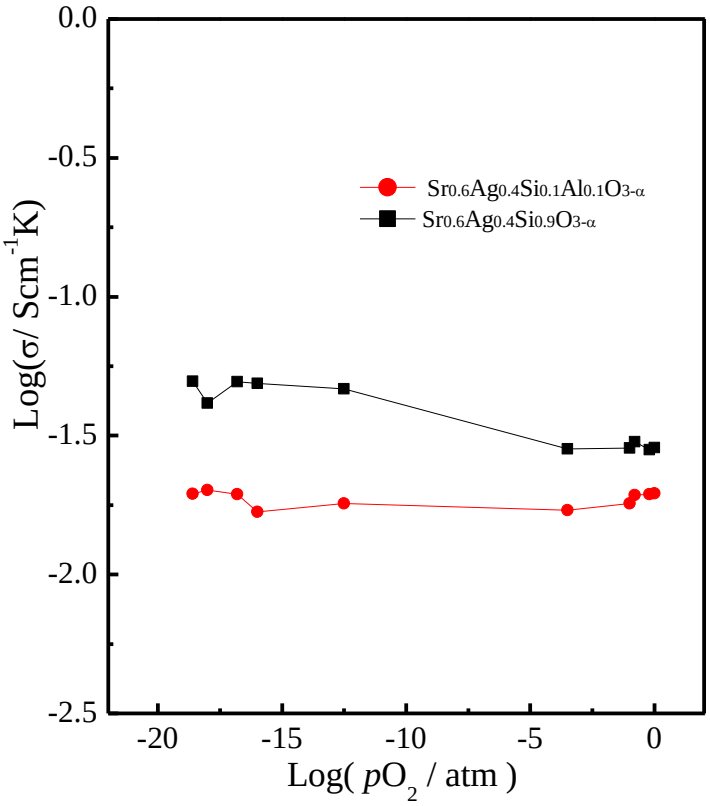


**Figure 5.**The conductivities of $Sr_{0.6}Ag_{0.4}SiO_{3-\alpha}$ and $Sr_{0.6}Ag_{0.4}Si_{0.9}Al_{0.1}O_{3-\alpha}$ vs. oxygen partial pressures ($pO_2$= $10^{-20}$ -1 atm) at 800 °C.

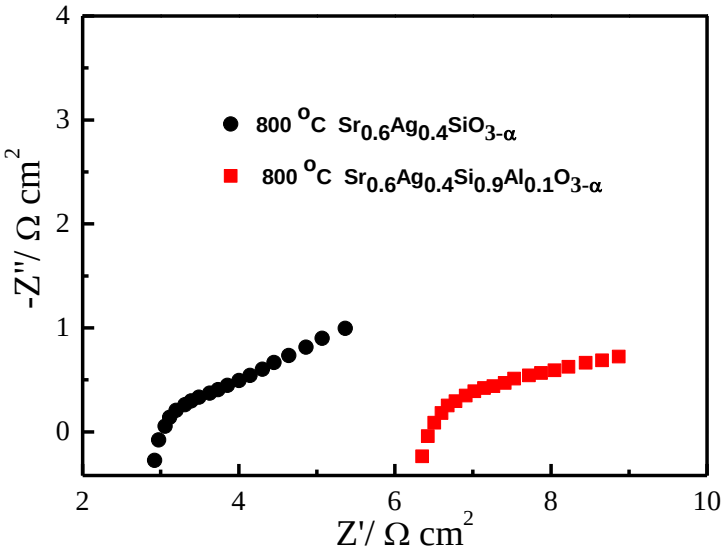


**Figure 6.** Impedance spectra of $Sr_{0.6}Ag_{0.4}SiO_{3-\alpha}$ and $Sr_{0.6}Ag_{0.4}Si_{0.9}Al_{0.1}O_{3-\alpha}$ under an open circuit condition at 800 °C.

Fig. 6 shows the impedance spectra of $Sr_{0.6}Ag_{0.4}SiO_{3-\alpha}$ and $Sr_{0.6}Ag_{0.4}Si_{0.9}Al_{0.1}O_{3-\alpha}$ under an open circuit condition at 800 °C. There are no clear semicircles, which may be due to the high resistances of the samples. We obtained the total resistance from the intercept of the linear region of

the curve to the real axis [27–29]. $^{23}Na$ solid state NMR investigation demonstrated that $Na^+$ ions in $Sr_{0.60}Na_{0.40}SiO_{2.80}$ are highly mobile and are responsible for the high conductivity. Substitution of $Si^{4+}$ with low valence $Al^{3+}$ ion in a tetrahedral position induces a negative charge which needs to be balanced by intercalation of $Na^+$, decreases the mobility of charge carriers, and thus leads to the decrease of the electrical conductivity [22–24]. The resistance of $Sr_{0.6}Ag_{0.4}Si_{0.9}Al_{0.1}O_{3-\alpha}$ (6.45 $\Omega \cdot cm^2$) is higher than that of $Sr_{0.6}Ag_{0.4}SiO_{3-\alpha}$ (2.98 $\Omega \cdot cm^2$) under an open circuit condition.

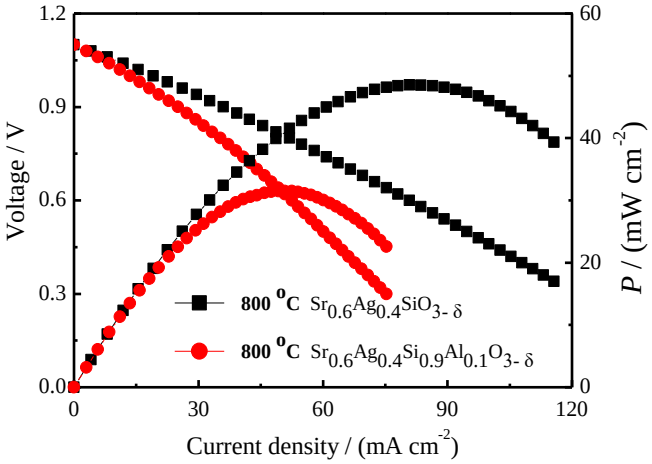


**Figure 7.** *I-V* and *I-P* curves for $H_2/O_2$ fuel cells using $Sr_{0.6}Ag_{0.4}SiO_{3-\alpha}$ and $Sr_{0.6}Ag_{0.4}Si_{0.9}Al_{0.1}O_{3-\alpha}$ at 800 °C.

The ampere density-voltage (*I-V*) and ampere density-power density (*I-P*) curves for $H_2/O_2$ fuel cells using $Sr_{0.6}Ag_{0.4}SiO_{3-\alpha}$ and $Sr_{0.6}Ag_{0.4}Si_{0.9}Al_{0.1}O_{3-\alpha}$ at 800 °C are shown in Fig. 7. Each cell has the same open circuit voltage (OCV) of 1.1 V, which indicates that the samples are dense. $Sr_{0.6}Ag_{0.4}SiO_{3-\alpha}$ shows the highest maximum power density of 48.5 $mW \cdot cm^{-2}$, which is 1.54 times higher than that of $Sr_{0.6}Ag_{0.4}Si_{0.9}Al_{0.1}O_{3-\alpha}$ at 800 °C. The highest maximum power densities of the samples are lower than that of $Sr_{3-3x}Na_{3x}Si_3O_{9-1.5x}$ (x = 0.45), as reported by Wei et al. [19]. This may be because the effect of sliver doping is low.

## 4. CONCLUSIONS

In this study, $Sr_{0.6}Ag_{0.4}SiO_{3-\alpha}$ and $Sr_{0.6}Ag_{0.4}Si_{0.9}Al_{0.1}O_{3-\alpha}$ electrolytes were synthesized via a high temperature solid state reaction method. The diffraction peaks at 17.50º, 30.59º, 35.44º and 63.72 belonged to the (002), (022), (004) and (044) of the perovskite structure of $SrSiO_3$, respectively. SEM photos showed that $Sr_{0.6}Ag_{0.4}SiO_{3-\alpha}$ and $Sr_{0.6}Ag_{0.4}Si_{0.9}Al_{0.1}O_{3-\alpha}$ pellets are well-sintered. The conductivities of $Sr_{0.6}Ag_{0.4}SiO_{3-\alpha}$ and $Sr_{0.6}Ag_{0.4}Si_{0.9}Al_{0.1}O_{3-\alpha}$ were $2.4\times10^{-2}$ $S \cdot cm^{-1}$ and $1.6\times10^{-2}$ $S \cdot cm^{-1}$ in a nitrogen atmosphere at 800 °C, respectively. The resistances of $Sr_{0.6}Ag_{0.4}Si_{0.9}Al_{0.1}O_{3-\alpha}$ and $Sr_{0.6}Ag_{0.4}SiO_{3-\alpha}$ were 6.45 $\Omega \cdot cm^2$ and 2.98 $\Omega \cdot cm^2$ under an open circuit condition, respectively. $Sr_{0.6}Ag_{0.4}SiO_{3-\alpha}$ showed the highest maximum power density of 48.5 $mW \cdot cm^{-2}$at 800 °C.

ACKNOWLEDGEMENTS
This work was supported by the National Natural Science Foundation (No. 51402052) of China, the Natural Science Foundation of Higher Education Institutions in Anhui Province (No. KJ2018A0337), Excellent Youth Foundation of Anhui Educational Committee (No. gxyq2018046), Horizontal cooperation project of Fuyang municipal government and Fuyang Normal College (No. XDHX2016019, XDHXTD201704).

## References

1. G. L. Liu, W. Liu Q. Kou and S. J. Xiao, *Int. J. Electrochem. Sci*., 13 (2018) 2641.
2. Y. Yang,H. Hao,L. Zhang,C. Chen,Z. Luo,Z. Liu,Z. Yao,M. Cao andH. Liu,*Ceram. Int.*, 44 (2018) 11109.
3. Y. N. Chen, T. Tian, Z. H. Wan, F. Wu, J. T. Tan and M. Pan, *Int. J. Electrochem. Sci.*, 13 (2018) 3827.
4. T. Hibino, K. Kobayashi, P. Lv, M. Nagao, S. Teranishi, and T. Mori,*J. Electrochem. Soc.*,164 (2017) F557.
5. S. Lee, and X. Guan,*MRS Communications.*, 7 (2017)199.
6. J. Luo, A.H. Jensen, N.R. Brooks, J. Sniekers, M. Knipper, D. Aili, Q. Li, B. Vanroy, M. Wübbenhorst, F. Yan, L.V. Meervelt, Z. Shao, J. Fang, Z.-H. Luo, D.E.D. Vos, K. Binnemans, and J. Fransaer,*Energy Environ. Sci.*,8 (2015) 1276.
7. A.A. Solovyev, S.V. Rabotkin, A.V. Shipilova and I.V. Ionov,*Int. J. Electrochem. Sci*., 14 (2019) 575.
8. C. Xia, Z. Qiao, C. Feng, J. Kim, B. Wang and B. Zhu, *Materials*, 11(2018) 40.
9. Y. Tian, Z. Lü, X. Guo and P. Wu,*Int. J. Electrochem. Sci*., 14 (2019) 1093.
10. H.-S. Kim, H.B. Bae, W.C. Jung and S.-Y. Chung, *Nano. Lett.*18(2018) 1110.
11. Z. Gong, W. Sun, Z. Jin, L. Miao and W. Liu, *ACS Appl. Energy Mater.*1(2018) 3521.
12. Z. Zhang, L. Chen, Q. Li, T. Song, J. Su, B. Cai and H. He, *Solid State Ionics* 323 (2018) 25.
13. X. Fang, J. Zhu and Z. Lin, *Energies*. 11 (2018) 1735.
14. M. A. Haque, A. B. Sulong, E. H. Majlan, K. S. Loh, T. Husaini and R. Rosli,*Int. J. Electrochem. Sci*., 14 (2019) 371.
15. C. Bernuy-Lopez, L. Rioja-Monllor, T. Nakamura, S. Ricote, R. O'Hayre, K. Amezawa, M. Einarsrud and T. Grande, *Materials*11 (2018) 196.
16. S. AjithKumar,P. Kuppusami and P.Vengatesh,*Ceram. Int.*44 (2018) 21188.
17. Y. Wan, B. He, R. Wang, Y. Ling and L. Zhao, *J. Power Sources*347 (2017) 14.
18. P. Singh and J.B. Goodenough,*J. Am. Ceram. Soc.*135 (2013) 10149.
19. T. Wei, P. Singh, Y. Gong, J.B. Goodenough, Y. Huang and K. Huang, *Energy Environ. Sci.* 7 (2014) 1680.
20. C.Tealdi, L. Malavasi, I. Uda, C. Ferrara, V. Berbenni and P. Mustarelli, *Chem. Commun.*50 (2014) 14732.
21. J. Xu, X. Wang, H. Fu, C.M. Brown, X. Jing, F. Liao, F. Lu, X. Li, X. Kuang and M. Wu, *Inorg. Chem.*53 (2014) 6962.
22. Y. Jee, X. Zhao and K. Huang, *Chem. Commun.*51(2015) 9640.
23. K.K. Inglis, J.P. Corley, P. Florian, J. Cabana, R.D. Bayliss and F. Blanc, *Chem. Mater.*28 (2016) 3850.
24. P.-H. Chien, Y. Jee, C. Huang, R. Dervisoglu, I. Hung, Z. Gan, K. Huang and Y.-Y. Hu, *Chem. Sci.*7 (2016) 3667.
25. F. Yang, Z. Yu, B. Meng, Y.J. Zhu, Q.Q. Yang, Z.L. Lin, H.M. Zhou and X. L. Liang,*Ionics*22 (2016) 2087.
26. A. Pandey, U.K. Chanda, L. Besra, K.K. Sahu, A. Roy and S. Pati, *J. Electroceram.*40(2017) 50.

27. R. Pandey, M. Viviani, P. Singh, R. Botter, M.P. Carpanese, A. Barbucci and S. Presto, *Solid State Ionics*314 (2018) 172.
28. A.K. Chandrappa, L.R. Potnuru and P.C. Ramamurthy, *J. Alloy. Compd.*745 (2018) 555.
29. J.T.S. Irvine, D.C. Sinclair and A.R. West, *Adv. Mater.* 2 (1990) 132.